Theoretical Model and Experimental Study of Slurry Erosion by Flowing Dilute Sulfuric Acid Under Turbulent Conditions

Weihang ZHANG, Zhigang SONG*

Abstract: Sewage pipes and acid rain, as the surface of concrete materials in buildings, are often eroded by sulfuric acid turbulence. In this paper, the influence of sulphuric acid with different velocity on the erosion rate of concrete mortar under turbulent conditions is studied. The thickness expression of the viscous inner layer is obtained by using the turbulent boundary layer theory, and the relationship between the viscous inner layer and the concentration boundary layer (CBLr) in the acidic solution near the mortar wall is established by using the Schmidt number. On this basis, a theoretical model of the relationship between the velocity of sulfuric acid and the erosion rate of mortar under turbulent conditions is derived, combining with the dissolution reaction process of dilute sulfuric acid erosion mortar (DSAEM). The results show that the erosion rate increases with the increase of the velocity, but decreases with the exponential relation of the velocity. In order to verify the rationality of the theoretical model, a simulated flow erosion test device was used to test 10 groups of cement mortar specimens for 800 h, and the experimental data of erosion rate and dilute sulfuric acid consumption of mortar specimens with water-binder ratio of 0.5, pH value of 3.4 and flow rate of 1.70 m/s ~ 2.87 m/s were obtained, and compared with the theoretical model. The experimental results show that the relationship between the amount of flushing and the flow rate is in good agreement with the theoretical results.

Keywords: cement mortar; flow corrosion model; sulfuric acid; turbulence

1 INTRODUCTION

With the widespread use of concrete materials and the acceleration of industrialization, the aging of concrete caused by sulfuric acid erosion has gradually become a global problem [1-5]. In sulfuric acid erosion, there are both static sulfuric acid erosion and flowing sulfuric acid erosion [6-9]. The concrete surface of buildings affected by sewage pipes and acid rain is often eroded by flowing sulfuric acid [10, 11], and the flow state of sulfuric acid is mostly in turbulent state and rarely in laminar flow state [12, 13]. Flowing sulfuric acid corrosion is often found in concrete sewer lines. The Design Code for Sewage Works (GB50014-2006) [14] and the European standard (EN12056-2000) [15] stipulate that the minimum design flow rate of sewers is 0.6 m/s to 5 m/s, and the minimum diameter size of concrete pipes is 0.2 m. Therefore, the minimum Reynolds number is 67000. In sewer pipes, the critical Reynolds number (Re_c) is 2320 [14], so the flow of sewage is usually turbulent. Sand et al. [15] monitored concrete corrosion in the Hamburg sewer system and observed corrosion rates at corrosion depths exceeding 6 mm/yr. Mori et al. [16] pointed out that the most severe corrosion occurred in the concrete area near the sewage level, with a corrosion rate of 5.7 mm/yr. Wells [17] and Bock [18] argued that several factors affect the corrosion rate, such as H2S concentration, temperature, pH, and the fluidity of acidic solutions. Some researchers have conducted many experimental and theoretical studies on the first three factors [19-23], but few studies have dealt with the effect of acidic solution mobility. Xiong et al. [24] studied the flow sulfuric acid erosion of four kinds of mortar, and the results showed that the flow sulfuric acid erosion was much more serious than static erosion.

Based on the boundary layer theory, a theoretical model of the relationship between sulfuric acid velocity and mortar erosion velocity under turbulent conditions was studied [25]. Firstly, the thickness expression of the viscous inner layer is obtained by applying the turbulent boundary layer theory, and the relationship between the viscous inner layer and the CBLr near the mortar wall is

established by using Schmidt number. On this basis, combined with the dissolution reaction process of DSAEM, the relationship between the velocity in the CBLr and the concentration gradient of dilute sulfuric acid was deduced [26]. The analytical functions of sulfuric acid flow rate and mortar erosion rate under turbulent conditions are derived, and the analytical functions of corrosion with time under different sulfuric acid flow rate are further given. In order to verify the rationality of the theoretical model, 10 groups of cement mortar specimens were tested for 800h with a simulated flow erosion test device. The experimental data of erosion rate and consumption of dilute sulfuric acid at pH 3.4 and flow rate of 1.70 m/s ~ 2.87 m/s for mortar with water-binder ratio of 0.5 were obtained, and compared with the theoretical model.

Sulfate ions start from the outside to react with some components of concrete, penetrate concrete, corrosion concrete, and then reduce the performance of concrete. The whole process is mainly influenced by two factors. First, the properties of concrete itself are called material factors. Including concrete water-cement ratio, porosity, cement type and dosage, aggregate type and grade, admixture and so on. The second is the characteristics of sulphate erosion environment of concrete production, called environmental factors. It includes the type of cation in the solution, the concentration of sulfate ions, the temperature of the solution, and the pH of the erosion solution. Material factors affect sulfate erosion mainly by influencing concrete compactness and the content of calcium aluminate hydrate and Ca (OH)$_2$. Studies have shown that the higher the concrete compactness, the lower the calcium aluminate hydrate content and the better the concrete resistance to sulfate attack. However, the degree of compaction and the content of calcium aluminate hydrate do not affect the mechanism of sulfate attack on concrete. Environmental factors affect the degradation rate of concrete mainly by influencing the condition or mechanism of sulfate reaction. Because the sulfate ions in groundwater and soil are different, the temperature is different, and the pH value is different, if the water level changes, the concrete will still

be in a state of dry and wet circulation. Therefore, concrete forms damaged by sulfate erosion in actual engineering are not the same. The influence of sulphate attack environmental factors on the degradation of concrete properties is very important. There are some literatures at home and abroad. Based on the mechanism of sulfate erosion and degradation of concrete materials, this paper summarizes the research results and weak links of environmental factors on sulfate erosion from a practical point of view based on reading a lot of domestic and foreign literature. The emphases and methods of concrete sulfate erosion research are put forward.

2 CORROSION MODEL OF MORTAR IN FLOWING SULFURIC ACID
2.1 TVBL and CBLr

When dilute sulfuric acid flows over the outsides of mortar, a velocity gradient presents in the turbulent velocity boundary layer (TVBL). TVBL in turbulence is divided into two layers. They are respectively the viscous bottom layer and the turbulent core layer (TCL) near the surface of the mortar [25]. In the viscous bottom layer, the flow state of sulfuric acid is laminar, and mass transfer should depend on the concentration gradient. According to Blasius [26], the thickness of the viscous bottom layer $\delta_b(u)$ can be expressed as follows.

$$\delta_b(u) = 72.2L^{0.1}(v/u)^{0.9} \tag{1}$$

In the above formula, u represents the fluid velocity (m/s), L represents the characteristic size of the pipeline (m), and v represents the coefficient of kinematic viscosity (m²/s), respectively.

At the same time, due to the different reaction at the interface between mortar and sulfuric acid, the mass transfer rate also has a concentration gradient perpendicular to the flow direction. Therefore, when dilute sulfuric acid flows through the mortar surface, two boundary layers appear simultaneously on the mortar surface. They are the TVBL and the CBLr (Fig. 1). According to Schmidt's law, the relationship between the thickness $\delta_b(u)$ of the CBLr in turbulent flow and the thickness $\delta_c(u)$ of the viscous bottom layer is as follows [28].

$$\delta_c(u)/\delta_b(u) = Sc^{-1/3} \tag{2}$$

Where Sc is Schmidt number. In TCL, the flow state of sulfuric acid is turbulent, and mass transfer mainly depends on eddy motion. Combining Eq. (1) and Eq. (2), we can have the following relationship.

$$\delta_c(u) = 72.2u^{-0.9}Sc^{-1/3}v^{0.9}L^{0.1} \tag{3}$$

According to Eq. (3), the CBLr thickness will decrease with the growth of liquid flow rate, which will cause the concentration gradient of sulfuric acid to thicken and the diffusion flux to increase. Therefore, it can ultimately enhance the corrosiveness of dilute sulfuric acid.
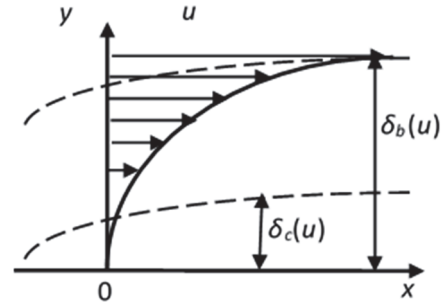

Figure 1 Concentration boundary layer and flow boundary layer

2.2 DSAEM Process

The DSAEM chemical reactions in the hydration products of cement mortar are dissolved and consumed by acid. CBLr surface is shown in Fig. 2. Since the equivalence ratio of the reaction is 1:1, DSAEM process modeled by the second-order homogeneous chemical reaction-diffusion equation of OH- in CBLr.

$$\frac{\partial M_{OH^-}(x,q)}{\partial q} = D_{OH^-}\frac{\partial^2 M_{OH^-}(x,q)}{\partial x^2} - kM_{OH^-}(x,q)M_{H^+}(x,q) \tag{4}$$

Where x is the distance to the fresh surface (m), q is the reaction time (s), $M_{OH^-}(x,q)$ and $M_{H^+}(x,q)$ are the concentrations of OH– and H+ at time q and position x (mol/L), respectively, D_{OH^-} is the diffusion coefficient of OH^- in the boundary layer (m²/s), and k is the reaction constant (mol⁻¹s⁻¹).

The boundary conditions are as follows.

$$\begin{cases} x=0, M_{OH^-}(0,q)=M_{OH^-,S}, M_{H^+}(0,q)=0 \\ x=\delta(q), M_{OH^-}(\delta(q),q)\approx 1\%M_{OH^-,S}, M_{H^+}(\delta(q),q)\approx 99\%M_{H^+,S} \end{cases} \tag{5}$$

Where $M_{OH^-,S}$ is the concentration of OH⁻ in Ca(OH)₂ and $M_{H^+,S}$ saturated solution, which is the H⁺ concentration in dilute sulfuric acid. $\delta(q)$ is the thickness of boundary layer, which can be defined as a distance where concentration reduce to 1% initial concentration.
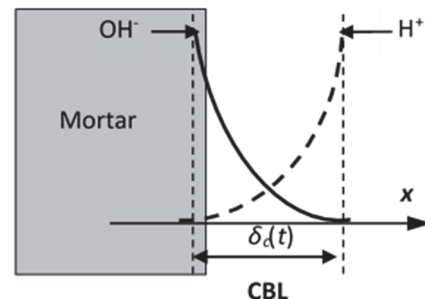

Figure 2 Concentration boundary layer between acid and mortar

2.3 Solution Under Flowing Acid Conditions

It can be assumed that the concentration distributions of H⁺ and OH⁻ can be assumed satisfy the following form.

$$M_{OH^-}(x, q) = M_{OH^-, S}\,e^{(-Fx/\delta(q))}$$

$$M_{H^+}(x, q) = M_{H^+, S}\left[1 - e^{-(Fx/\delta(q))}\right]$$

(6)

Combined Eq. (4) and Eq. (6), we can get the following relationship.

$$\frac{Fx}{\delta(q)^2}\frac{d\delta(q)}{dq} = D_{OH^-}F^2\Big/\delta(q)^2 - kM_{H^+, S}\left[1 - e^{(-Fx/\delta(q))}\right]$$

(7)

Eq. (7) integrates both sides simultaneously, with an interval of 0 to $\delta(q)$ Rearranging can lead to the following relationship.

$$\ln\left\{4D_{OH^-}F^2 - \left[4kM_{H^+, S}\delta(q)^2\left(F + e^{(-F)} - 1\right)\right]\Big/F^2\right\} =$$
$$= -\left[4kM_{H^+, S}t\left(F + e^{(-F)} - 1\right)\right]\Big/F^2 + M$$

(8)

Based on the initial conditions $q = 0$ and $\delta(q) = 0$, we can get $M = \ln\{4D_{OH^-}F^2$. In addition, substituting M into the Eq. (8) can have the following relationship:

$$\delta(q) = \sqrt{4F^2 D_{OH^-}\left\{1 - e^{\left[-\left(4kM_{H^+, S}q\left(F + e^{(-F)} - 1\right)\right)\Big/F^2\right]}\right\}}$$

(9)

The acid flow rate on the corrosion zone S is Eq. (10).

$$V_{H^+}(q, x) = D_{H^+}S\frac{\partial M_{H^+}}{\partial x}\bigg|_x =$$
$$= \left[D_{H^+}M_{H^+, S}Se^{(-Fx/\delta(q))}F\right]\Big/\delta(q)$$

(10)

According to Eq. (3), in the turbulent flow of acid, the CBLr thickness is $\delta_c(u)$. Thus, for $x = \delta_c(u)$, the acid consumption rate $V_{H^+}(q, x)$ can be expressed as Eq. (11).

$$V_{H^+}(q, \delta_c(u)) = \left[ae^{\left(-cu^{-0.9}\Big/\sqrt{1 - e^{(-bq)}}\right)}\right]\Big/\sqrt{1 - e^{(-bq)}}$$

(11)

where,

$$\begin{cases}a = D_{H^+}M_{H^+, S}S\Big/2\sqrt{D_{OH^-}} \\ b = 4kM_{H^+, S}\left(F + e^{(-F)} - 1\right)\Big/F^2 \\ c = 36.1Sc^{-1/3}v^{0.9}L^{0.1}\Big/\sqrt{D_{OH^-}}\end{cases}$$

(12)

From Eq. (11), $V_{H^+}(q)$ will increase with u due to q > 0. Further, for the flow velocity vL, the acid consumption rate $V_{H^+}(q)$ will reach at the value

$ae^{\left(-Mu^{-0.9}\right)}$ in Eq. (13), when reaction time nearly reach at the infinity.

$$V_{H^+}(q \to \infty) = D_{H^+}M_{H^+, S}Se^{\left(-5u^{-0.9}Sc^{-1/3}\sqrt{vL}\Big/2\sqrt{D_{OH^-}}\right)}\Big/2\sqrt{D_{OH^-}} =$$
$$= ae^{\left(-Mu^{-0.9}\right)}$$

(13)

According to Eq. (13), as the reaction time approaches infinity, the acid consumption rate $V_{H+}(q)$ tends towards a normal number. The stable acid consumption rate increases with the growth of flow rate. This value $ae^{\left(-Mu^{-0.9}\right)}$ is limited by the concentration of sulfuric acid during stable reaction, H+ diffusion coefficient.

2.4 Acid Consumption

The integration of Eq. (14) from 0 to Q can obtain the acid consumption $M_{H^+}(Q)$.

$$M_{H^+}(Q) = \int_0^Q V_{H^+}(q, \delta_c)dq =$$
$$= \int_0^Q \left[ae^{\left(-Mu^{-0.9}\Big/\sqrt{1 - e^{(-bq)}}\right)}\right]\Big/\sqrt{1 - e^{(-bq)}}\,dq$$

(14)

Since the integration of Eq. (14) is not easy, a second-order expansion of the velocity influence term approximates the velocity influence term.

$$V_{H^+}(q, \delta_m(n)) \approx$$
$$\approx \frac{a}{\sqrt{1 - e^{(-bq)}}}\left[1 - \left(mn^{-0.9}\Big/\sqrt{1 - e^{(-bq)}}\right) + \frac{1}{2}\left(mn^{-0.9}\Big/\sqrt{1 - e^{(-bq)}}\right)^2\right] =$$
$$= \frac{a}{\sqrt{1 - e^{(-bq)}}} - \frac{amn^{-0.9}}{1 - e^{(-bq)}} + \frac{am^2 n^{-1.8}}{2\left[1 - e^{(-bq)}\right]^{1.5}}$$

(15)

Substitute Eq. (15) into Eq. (14), and integrating both sides of Eq. (14), we can obtain the total acid consumption $M_{H+}(Q)$ within Q.

$$W_{H^+}(Q) = \int_0^Q V_{H^+}(q, \delta_m)dq \approx \int_0^Q \left(\frac{a}{\sqrt{1 - e^{(-bq)}}} - \frac{amn^{-0.9}}{1 - e^{(-bq)}} + \frac{am^2 n^{-1.8}}{2\left[1 - e^{(-bq)}\right]^{3/2}}\right)dq =$$
$$= \frac{2a}{b}\ln\left[\frac{1 + \sqrt{1 - e^{(-bQ)}}}{1 - \sqrt{1 - e^{(-bQ)}}}\right] - \frac{amn^{-0.9}}{b}\ln\left(\left[e^{(-bQ)} - 1\right]\Big/\left[e^{(-bQ)}\right]\right) +$$
$$+ \frac{amn^{-1.8}}{b}\left\{\ln\left[\left(\sqrt{1 - e^{(-bQ)}} + 1\Big/\sqrt{1 - e^{(-bQ)}} - 1\right)\right] - 2\Big/\sqrt{1 - e^{(-bQ)}}\right\} =$$
$$= A(Q) - B(Q)n^{-0.9} + C(Q)n^{-1.8}$$

(16)

Where,

$$\begin{cases}A(Q) = \frac{2a}{b}\ln\{(1 + \sqrt{1 - e^{(-bQ)}})\,/\,(1 - \sqrt{1 - e^{(-bQ)}})\} \\ B(Q) = \frac{am}{b}\ln\left(\left[e^{(-bQ)} - 1\right]\Big/\left[e^{(-bQ)}\right]\right) \\ C(Q) = \frac{am}{b}\left\{\ln\left[\left(\sqrt{1 - e^{(-bQ)}} + 1\Big/\sqrt{1 - e^{(-bQ)}} - 1\right)\right] - 2\Big/\sqrt{1 - e^{(-bQ)}}\right\}\end{cases}$$

(17)

As shown in Eq. (16), as the flow rate approaches infinity, the acid consumption $M_{H^+}(Q)$ will approach $A(Q)$. That is, the amount of corrosion does not always increase with the flow rate, and there is the maximum limit value.

3 EXPERIMENT
3.1 Materials

According to reference [20], 10 cylindrical cement mortar samples (diameter 50 mm × height 100 mm) were manufactured. The mixed materials include Portland cement (P.0.43 grade), Chinese ISO standard distilled water and mix ratios as shown in Tab. 1.

3.2 Flow-Corrosion Devices

When the Scientific Research Institute of Kunming Railway Bureau in China studied the sulfate erosion damage problem of Chengdu-Kunming railway engineering concrete, it used the accelerated test method of dry and wet cycle and the method of immersion in the field to carry out comparative tests [11]. Their test pieces have three sizes, namely 7 cm × 7 cm × 21 cm prism, 4 cm × 4 cm × 16 cm prism and 7.07 cm × 7.07 cm cube. The dry and wet cycle system is as follows, room temperature soaking for 14 hours remove and wipe the surface water for 1 hour –80 °C constant temperature drying for 6 hours cooling observation for 1 hour, that is, a cycle, each cycle is 24 hours. The results of the dry and wet cycle method were compared with the results of long-term immersion in the field, and they found that the two methods had a good agreement. This paper independently developed and produced a flow corrosion device. The main equipment consists of an electric rotary engine, water tank, energy dissipation network and a governor, as shown in Fig. 3. With the controller, the unit can provide a range of rotational linear speeds from 0 m/s to 3.7 m/s. The critical Reynolds count ($CRec$) for the transition flow ranges from 1.6×10^5 to 3.6×10^5 [18].

$$Re_m = n_m L / v \tag{18}$$

In this formula, the characteristic size of sample L is 0.0157 m. At 20 °C and standard atmosphere, the kinetic viscosity coefficient of sulfuric acid is 1.00374×10^{-6} m^2/s, and the critical flow rate ranges from 0.9 m/s to 2.22 m/s. The linear rotation velocity of the selected samples in this experiment ranges from 1.7 m/s to 2.87 m/s, which belongs to turbulence.
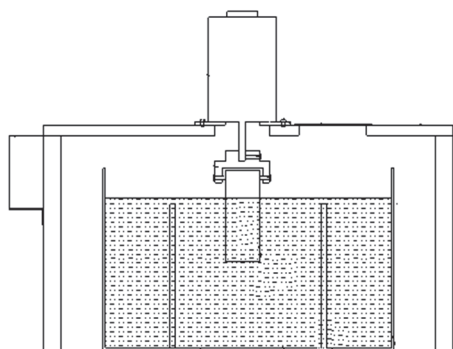

Figure 3 Flow-corrosion device

3.3 Experimental Arrangement

According to GBT 17671-2021 in China, 10 sets of cylindrical mortar specimens with diameter of 0.05 m and height of 0.1 m were made in this paper. The mixing ratio (mass ratio) of the specimen is 0.5. The erosion solution is dilute sulfuric acid with 3.4 pH Value. The specific experimental arrangements are shown in Tab. 1. After vibration molding, the specimen was placed in a standard curing box (constant temperature 24 °C, relative humidity 0.88) for 24 hours. After stripping, it was cured in saturated sodium hydroxide solution for 28 days. After curing, it was naturally dried in the room for 1 week. In order to avoid direct contact between the top of the sample and the bearing clamp and eliminate the influence of dilute sulfuric acid washing from the bottom of the sample, the paper uses polyethylene-based resin to seal both ends of the sample, leaving only one side of the cylindrical sample to interact with dilute sulfuric acid, as shown in Fig. 4. After the experiment began, the pH value of the acid solution was observed in real time with pHB – 1 pH meter (accuracy 0.01). At the same time, 0.13 mol/L dilute sulfuric acid was titrated to maintain the pH value. The consumption rate of dilute sulfuric acid can be obtained by dividing the amount per drop by the interval time per drop as follows.

$$V_{Hi} = V_i \left(q_i - q_{i-1} \right)^{-1} \tag{19}$$

Where, q_{i-1} and q_i is the time of the $(i-1)$th and ith titration respectively. V_i is volume consumption of titration acid (concentration 0.13 mol/L) in ith titration. V_{Hi} is the average reaction rate from time q_{i-1} to q_i.
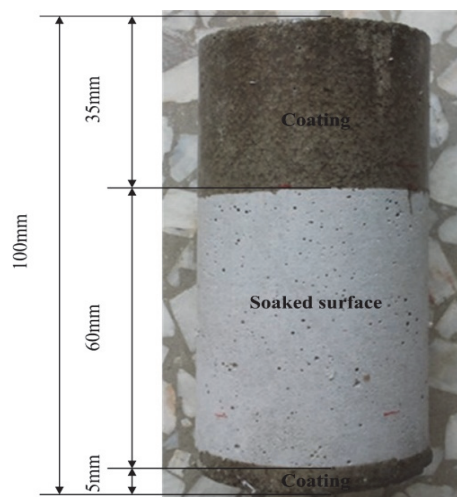

Figure 4 Cement mortar specimen

Table 1 Mix proportion, pH value of solution and velocity

Group	mw/mc	Mix proportion (by mass)			pH	Velocity / m/s
		S	C	W		
1	0.5	3	1	0.5	3.4	1.70
2	0.5	3	1	0.5	3.4	1.83
3	0.5	3	1	0.5	3.4	1.96
4	0.5	3	1	0.5	3.4	2.09
5	0.5	3	1	0.5	3.4	2.22
6	0.5	3	1	0.5	3.4	2.35
7	0.5	3	1	0.5	3.4	2.48
8	0.5	3	1	0.5	3.4	2.61
9	0.5	3	1	0.5	3.4	2.74
10	0.5	3	1	0.5	3.4	2.87

3.4 Results and Discussion
3.4.1 Acid Consumption MH + (Q)

Tab. 2 shows the total acid consumption after 200 hours, 400 hours, 600 hours and 800 hours. The corresponding A(Q), B(Q) and C(Q) fitting degrees of Eq. (16) are shown in Tab. 3. The fitting curve is shown in Fig. 5. It is found that Eq. (16) has a very high fitting degree. The results show that the experimental relationship between acid consumption and velocity is in good agreement with the theoretical model.

Table 2 Specimen Acid consumption at different stages

Group	u / m/s	$M_{H+}(Q)$ / mmol			
		200 h	400 h	600 h	800 h
1	1.70	67.3	87.5	101.5	112.4
2	1.83	73.8	94.1	108.5	118.2
3	1.96	76.0	96.6	110.8	121.6
4	2.09	78.6	98.7	112.6	123.3
5	2.22	79.6	99.6	113.4	124.3
6	2.35	81.7	101.6	116.3	127.3
7	2.48	83.4	103.5	117.5	128.5
8	2.61	86.0	106.3	120.6	131.4
9	2.74	87.7	107.9	122.1	133
10	2.87	88.1	108.7	123.4	134.2

Table 3 Regression experimental results according to Eq. (16)

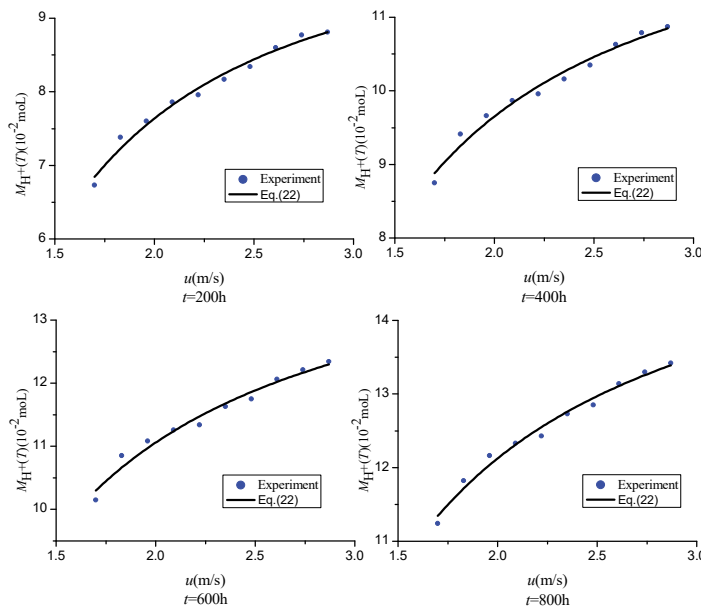| Time	A(Q)	B(Q)	C(Q)	Correlation coefficient
200 h	10.50	1.81	−6.58	0.978
400 h	13.01	3.80	−4.60	0.972
600 h	14.93	5.70	−2.85	0.966
800 h	16.02	5.50	−3.22	0.980

Figure 5 Acid consumption and fitting curves of the specimen at different times

3.4.2 Acid Consumption Rate VH + (q)

According to Eq. (11), the acid consumption rate and the rate obtained from the curve fitted by the analytical solution are shown. Tab. 4 shows that the results of a, b and c are also different under different groups of flow rates. The fitting curve is shown in Fig. 6. We found the equation. Eq. (11) shows that the fitting correlation coefficient is greater than 0.9 that is, the fitting degree is very high.

Table 4 Regression experimental results according to Eq. (11)

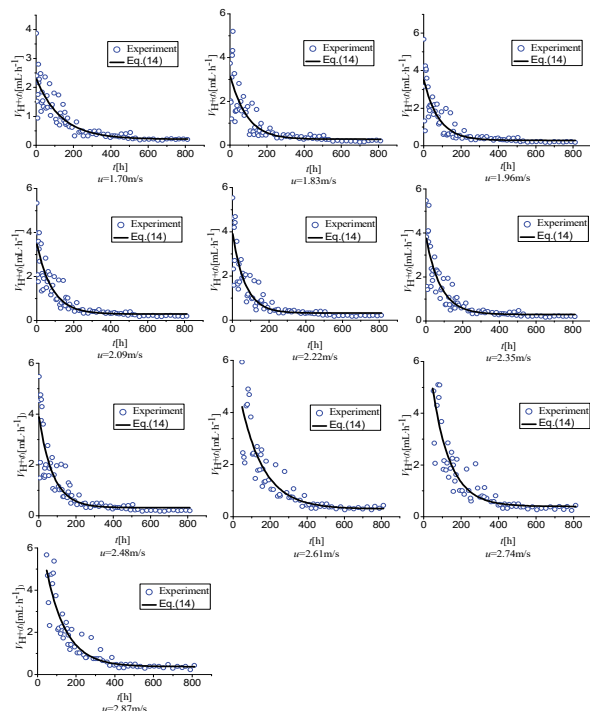| Index	$a \times 10^3$ / m³mol/h1/2mL	$b \times 10^7$ / h−1mL−1	$c \times 10^4$ / m1/2	Correlation coefficient
1	17.96	2.73	21.75	0.928
2	12.65	0.88	13.62	0.926
3	13.17	1.52	9.48	0.901
4	12.06	0.96	8.37	0.979
5	8.71	0.46	5.42	0.937
6	12.01	0.79	8.62	0.926
7	9.88	0.54	6.53	0.951
8	12.17	0.71	8.74	0.927
9	10.32	0.52	5.45	0.947
10	13.09	0.76	7.84	0.959

Figure 6 Acid consumption rate and fitting curves of different groups

4 CONCLUSION

Based on viscous bottom layer and CBLr model, a theoretical model of the relationship between mortar corrosion rate and sulfuric acid corrosion is proposed and verified by corresponding experimental analysis. Finally, the following conclusions are drawn.

a) The corrosion rate is positively correlated with the flow rate, but the incremental rate decreases with the increase of flow rate. The initial setting time and final setting time of super sulfur cement is longer than that of ordinary Portland cement.

b) When the sulfuric acid flow rate increases to a certain range, the corrosion rate reaches the upper limit. The upper limit of corrosion rate is determined by the factors, which are the sulfuric acid concentration, OH– the diffusion coefficient and the mortar corrosion area.

c) According to the test results, the test results of corrosion rate and flow rate are completely consistent with the analytical model proposed in this paper.

Acknowledgements

5 REFERENCES

[1] Martin, D. E. (1991). Acid Rain and Air Pollution viscous bottom layer the Building and Outdoor Sculptures of Montreal. *ART XXIII-45*, 13-19. https://doi.org/10.2307/1504363

[2] Pavlik, V. (2007). Degradation of Concrete by Flue Gases from Coal Combustion. *Cement and Concrete Research, 37*(7), 1085-1095. https://doi.org/10.1016/j.cemconres.2007.04.008

[3] Lee, H. & Cody, R. D. (2005). The Formation and Role of Ettringite in Iowa Highway Concrete Deterioration. *Cement and Concrete Research, 35*(1), 332-343. https://doi.org/10.1016/j.cemconres.2004.05.029

[4] Belie, D. & Monteny, J. (2004). Experimental Research and Prediction of the Effect of Chemical and Biogenic Sulfuric Acid on Different Types of Commercially Produced Concrete Sewer Pipes. *Cement and Concrete Research, 34*(2), 323-336. https://doi.org/10.1016/j.cemconres.2004.02.015

[5] Rosso, F., Jin, W., & Pisello, A. L. (2016). Translucent marbles for building envelope applications: Weathering effects on surface lightness and finishing when exposed to simulated acid rain. *Construction and Building Materials, 108*, 146-153. https://doi.org/10.1016/j.conbuildmat.2016.01.041

[6] Du, Y. J., Wei, M. L., Reddy, K. R., Liu, Z. P., & Fei, J. (2014). Effect of acid rain pH on leaching behavior of cement stabilized lead-contaminated soil. *Journal of hazardous materials, 14*(271), 131-140. https://doi.org/10.1016/j.jhazmat.2014.02.002

[7] Fan, Y., Zhang, S., Wang, Q., & Shah Surendra, P. (2016). The effects of nano-calcined kaolinite clay on cement mortar exposed to acid deposits. *Construction and Building Materials, 102*, 486-495. https://doi.org/10.1016/j.conbuildmat.2015.11.016

[8] Chidiac, P. D. K. (2008). Evolution of mechanical properties of concrete containing ground granulated blast furnace slag and effects on the scaling resistance test at 28days. *Cement and Concrete Composites, 30*(2), 63-71. https://doi.org/10.1016/j.cemconcomp.2007.09.003

[9] Livingston, R. A. (2016). Acid rain attack on outdoor sculpture in perspective. *Atmospheric Environment, 146*, 332-345. https://doi.org/10.1016/j.atmosenv.2016.08.029

[10] Song, Z. G. & Yang, X. S. (2011). Material Degradation of RC Structures Attacked by Acid Raina Field Investigation in Kunming. *Concrete, 11*(7), 23-27.

[11] DKB. (1972). Thistlethwayte, Control of sulphides in sewerage systems. *Butterworth, 7*, 43-51

[12] Xie, S. D. & Li, D. (2004). Investigation of the Effects of Acid Rain on the Deterioration of Cement Concrete Using Accelerated Tests Established in Laboratory. *Atmospheric Environment, 38*(4), 457-466. https://doi.org/10.1016/j.atmosenv.2004.05.017

[13] Bohm, M. & Devinny, J. S. (1998). On a Moving-Boundary System Modeling Corrosion in Sewer Pipes. *Applied Mathematics and Computation, 92*(8), 247-269. https://doi.org/10.1016/S0096-3003(97)10039-X

[14] Liu, J. & Vipu, D. (2007). Modeling water and sulfuric acid transport through coated cement concrete. *Journal of engineering mechanics, 129*(4), 426-437. https://doi.org/10.1061/(ASCE)0733-9399(2003)129:4(426)

[15] Song, Z. G. & Zhang, X. S. (2011). Concentration Boundary layer Model of Mortar Corrosion by Sulfuric Acid. *Journal of Wuhan University of Technology-Mater, 26*(3), 527-532. https://doi.org/10.1007/s11595-011-0262-9

[16] Schlichting, H. & Gersten. K. (2016). Extensions to the Prandtl Boundary–Layer Theory//Boundary-Layer Theory. *Springer Berlin Heidelberg, 17*(20), 377-411. https://doi.org/10.1007/978-3-662-52919-5_14

[17] Schlichting, H. & Gersten, K. Boundary-layer theory. *Springer, 29*(32), 527-532

[18] Min, H. G. (2010). Experimental research on the sulfate corrosion resistance of concrete and cement mortar. *Kunming University of Science and Technology, 10*(1), 28-31.

[19] Feng, J. & Yan, P. Y. (2017). Performance and microstructure of oil well cement stone after sulfuric acid corrosion. *Chinese Journal of Silicomium, 40*(05), 671-676.

[20] Zhigang, S. & Xue, S. (2010). Experimental study on corrosion of mortar by dilute sulfuric acid. *Chinese Journal of Building Materials, 15*(02), 163-167.

[21] Liu, J. & Vipulanandan, C. (2018). Modeling water and sulfuric acid transport through coated cement concrete. *Journal of engineering mechanics, 129*(4), 426-437. https://doi.org/10.1061/(ASCE)0733-9399(2003)129:4(426)

[22] Wells, T. & Melchers, R. E. (2015). Modelling concrete deterioration in sewers using theory and field observations. *Cement and Concrete Research, 77*(12), 82-96. https://doi.org/10.1016/j.cemconres.2015.07.003

[23] Song, Z. G. (2013). Concentration Boundary Layer Model of Mortar Corrosion by Sulfuric Acid. *Journal of Wuhan University of Technology-Mater, 26*(3), 527-532. https://doi.org/10.1007/s11595-011-0262-9

[24] Hewayde, H., Nehdi, M. E., & Allouche, E. (2014). Effect of geopolymer cement on microstructure, compressive strength and sulphuric acid resistance of concrete. *Magazine of Concrete Research, 58*(5), 321-331. https://doi.org/10.1680/macr.2006.58.5.321

[25] Sun, X., Jiang, G., & Bond, P. L. (2015). A novel and simple treatment for control of sulfide induced sewer concrete corrosion using free nitrous acid. *Water research, 70*(17), 279-287. https://doi.org/10.1016/j.watres.2014.12.020

[26] Etteyeb, N., Dhouibi, L., & Takenouti, H. (2014). Protection of reinforcement steel corrosion by phenyl phosphonic acid pre-treatment PART I: Tests in solutions simulating the electrolyte in the pores of fresh concrete. *Cement and Concrete Composites, 55*(24), 241-249. https://doi.org/10.1016/j.cemconcomp.2014.07.025

[27] Monteny, J. & Vincke, E. (2000). Biogenic and chemical sulfuric acid corrosion of mortars. *Cement and Concrete

Research, 11(4), 623-634.
https://doi.org/10.1016/S0008-8846(00)00219-2

Contact information:

Weihang ZHANG
Faculty of Civil Engineering, Kunming University of Science and Technology,
Kunming, China

Zhigang SONG
(Corresponding author)
Faculty of Civil Engineering, Kunming University of Science and Technology,
Kunming, China
E-mail: songzhigang_kust@163.com